Localization of epileptogenic zones in Lennox–Gastaut syndrome using frequency domain source imaging of intracranial electroencephalography: a preliminary investigation

2013 Physiol. Meas. 34 247

(http://iopscience.iop.org/0967-3334/34/2/247)

IOP Publishing Physiological Measurement

Physiol. Meas. **34** (2013) 247–263 doi:10.1088/0967-3334/34/2/247

Localization of epileptogenic zones in Lennox–Gastaut syndrome using frequency domain source imaging of intracranial electroencephalography: a preliminary investigation

Jae-Hyun Cho[1,5], Hoon-Chul Kang[2,5], Young-Jin Jung[1], Jeong-Youn Kim[1], Heung Dong Kim[2], Dae Sung Yoon[3], Yong-Ho Lee[4] and Chang-Hwan Im[1,6]

[1] Department of Biomedical Engineering, Hanyang University, Seoul, Korea
[2] Department of Pediatrics, Yonsei University College of Medicine, Seoul, Korea
[3] Department of Biomedical Engineering, Yonsei University, Wonju, Korea
[4] Korea Institute of Standard and Sciences (KRISS), Daejeon, Korea

E-mail: ich@hanyang.ac.kr

Received 9 August 2012, accepted for publication 13 December 2012
Published 28 January 2013
Online at stacks.iop.org/PM/34/247

Abstract

Although intracranial electroencephalography (iEEG) has been widely used to localize epileptogenic zones in epilepsy, visual inspection of iEEG recordings does not always result in a favorable surgical outcome, especially in secondary generalized epilepsy such as Lennox–Gastaut syndrome (LGS). Various computational iEEG analysis methods have recently been introduced to confirm the visual inspection results. Of these methods, high gamma oscillation in iEEG has attracted interest because a series of studies have reported a close relationship between epileptogenic zones and cortical areas with high gamma oscillation. Meanwhile, frequency domain source imaging of EEG and MEG oscillations has proven to be a useful auxiliary tool for identifying rough locations of epileptogenic zones. To the best of our knowledge, however, frequency domain source imaging of high gamma iEEG oscillations has not been studied. In this study, we investigated whether the iEEG-based frequency domain source imaging of high gamma oscillation (60–100 Hz) would be a useful supplementary tool for identifying epileptogenic zones in patients with secondary generalized epilepsy. The method was applied to three successfully operated on LGS patients, whose iEEG contained some ictal events with distinct high gamma oscillations before seizure onset. The resultant cortical source distributions were compared with surgical resection areas and with high gamma spectral power distributions on the intracranial sensor plane. While the results of the sensor-level analyses contained many spurious activities, the results of frequency domain source imaging coincided better with the surgical resection

[5] These authors contributed equally to this work.
[6] Author to whom any correspondence should be addressed.

areas, suggesting that the frequency domain source imaging of iEEG high gamma oscillations might help enhance the accuracy of pre-surgical evaluations of patients with secondary generalized epilepsy.

Keywords: source imaging, epileptogenic zone, high gamma oscillation, intracranial electroencephalography (iEEG), Lennox–Gastaut syndrome (LGS), secondary generalized epilepsy

(Some figures may appear in colour only in the online journal)

1. Introduction

Precise localization of epileptogenic zones is critical for successful surgical treatment of patients with intractable drug-resistant epilepsy. Traditionally, epileptogenic zones have been identified via various neuroimaging techniques such as electroencephalography (EEG), magnetoencephalography (MEG), intracranial EEG (iEEG), functional magnetic resonance imaging triggered by simultaneously recorded EEG, single photon emission computed tomography (SPECT), and positron emission tomography (PET) (Krakow *et al* 1999, Oliveira *et al* 1999, Kim *et al* 2002, Wu *et al* 2006). Among them, iEEG recorded from intracranial subdural grid or strip electrodes has been regarded as the most reliable modality for determining surgical resection areas prior to epilepsy surgery (Behrens *et al* 1994, Binnie *et al* 1994, Dubeau and McLachlan 2000, Rosenow and Lüders 2001, Pondal-Sordo *et al* 2007). Traditionally, identification of epileptogenic zones relied upon visual inspection of iEEG recordings by experienced epileptologists. For example, epileptogenic zones are usually found in locations with sustained rhythmic changes on electrocorticograms accompanied by subsequent clinically typical seizure activity. However, removal of epileptogenic zones identified using iEEG does not always guarantee a favorable surgical outcome (Prasad *et al* 2003, Boling *et al* 2009). Indeed, it is often difficult for even the most experienced epileptologists to distinguish ictal epileptogenic zones from irritative zones activated by propagation through visual inspection of ictal epileptiform activities.

In order to confirm the visual inspection results and further assist in making the final decision on surgical resection areas, various computational iEEG analysis methods have recently been introduced and used to identify epileptogenic zones of intractable epilepsies (Mars and Lopes da Silva 1987, Ding *et al* 2007, Swiderski *et al* 2009, Wilke *et al* 2010, Jung *et al* 2011). Among the various computational iEEG analysis methods, high gamma oscillations (60–100 Hz) have attracted considerable attention because recent studies demonstrated that cortical areas showing strong, high gamma spectral power before seizure onset coincided well with the primary epileptogenic foci (Allen *et al* 1992, Fisher *et al* 1992, Alarcon *et al* 1995, Traub *et al* 2001, Worrell *et al* 2004, Kobayashi *et al* 2009, Rampp *et al* 2010). According to a report by Fisher *et al* (1992), iEEG recordings acquired from patients with implanted subdural electrodes showed a two-fold increase in the spectral power of the frequency range between 40 and 50 Hz and a five-fold increase in the spectral power of the frequency range between 80 and 120 Hz, especially before the start of an epileptic seizure. Alarcon *et al* (1995) noted that localized high frequency activity (20–80 Hz) in iEEG recordings was associated closely with a good surgical outcome in patients with partial epilepsy. Traub *et al* (2001) reported that high frequency oscillations (HFOs) (>70 Hz) can precede the onset of seizures, and such activity can be superimposed on intra-seizure bursts as well as interictal bursts in pediatric epilepsy patients with focal cortical dysplasia (CD) and intractable seizures. Worrell *et al* (2004)

postulated that high frequency epileptiform oscillations (60–100 Hz) are clinically useful for localizing the epileptogenic zones in neocortical epilepsy, identifying periods of increased probability of seizure onset, and elucidating mechanisms underlying neocortical ictogenesis. Kobayashi *et al* (2009) investigated high gamma activities (peak frequency ranging from 43.0 to 101.6 Hz) in the ictal EEGs of tonic spasms and found that some tonic seizures might have the same generative mechanisms as epileptic seizures in patients with Lennox–Gastaut syndrome (LGS). A study by Rampp *et al* (2010) showed that MEG can also detect spike-locked and spike-independent high gamma oscillations and demonstrated that fast oscillations in frequency bands below 100 Hz are highly associated with epileptic networks. Consistent with previous studies, the high gamma oscillation analysis results shown in this study also corresponded to the surgical resection areas, especially better when the frequency domain iEEG source imaging was applied. To date, most of the published literature on high gamma oscillation focused on a sensor-level analysis. For example, epileptogenic zones were estimated by searching for iEEG sensors containing frequent or high power high gamma oscillations.

On the other hand, several research groups have recently reported that iEEG recordings could be used to estimate underlying 3D cortical sources with reasonable accuracy. They demonstrated that iEEG source imaging could provide auxiliary information about underlying brain activities associated with epilepsy, which eventually can be used for pre-surgical evaluation of intractable epilepsies (Fuchs *et al* 2007, Zhang *et al* 2008, Dümpelmann *et al* 2009, 2012, Cho *et al* 2011). In practice, misidentification of subdural grid or strip electrode locations can lead to incorrect or inaccurate localization of epileptogenic foci; however, iEEG source imaging has the potential to localize epileptogenic sources generated outside the subdural electrodes (Kim *et al* 2010). Moreover, iEEG source imaging results can be used to confirm the conclusions drawn from visual inspection of ictal or interictal iEEG recordings (Kim *et al* 2010), as defining and localizing epileptogenic zones can be difficult particularly when rapidly propagating epileptiform activities exist (Wilke *et al* 2010). Most importantly, the use of additional imaging modalities and imaging results should provide supplementary information for determining surgical resection areas.

In previous EEG and MEG studies, epileptogenic zones were sometimes identified using frequency domain source imaging, which estimated either locations of dipolar sources or distributions of cortical extended sources for a specific frequency band of interest (Lantz *et al* 1999, Worrell *et al* 2000, Xiang *et al* 2009). Frequency domain imaging of epileptogenic sources could provide important underlying information regarding epileptogenesis because in many practical cases the generation and propagation of epileptiform activities are known to be closely related to specific frequency bands, e.g. alpha and low-beta bands during ictal periods of some types of partial epilepsy (Lantz *et al* 1999, Worrell *et al* 2000) and a high gamma band before seizure onset (Xiang *et al* 2009). To the best of our knowledge, however, no studies have investigated the feasibility of frequency domain source imaging of iEEG recordings for the identification of epileptogenic sources.

In this study, we hypothesized that the frequency domain source imaging of iEEG high gamma band activity could provide useful additional information for the localization of epileptogenic zones in refractory epilepsy, which might not be obtained via the conventional sensor-level spectral analyses. We specifically focused on the localization of epileptogenic zones in secondary generalized epilepsy because it is generally difficult to localize epileptogenic zones of secondary generalized epilepsy due to their generalized ictal epileptic discharges. Among the various types of secondary generalized epilepsy, LGS was selected because this type of epilepsy requires accurate localization of epileptogenic zones for surgical treatment, but it is difficult to localize epileptogenic zones via visual inspection of ictal iEEG recordings. LGS is an epileptic syndrome with intractable, multiple

seizure types including tonic, atonic, myoclonic, and atypical absence seizures (Heiskala 1997). Some patients with LGS have focal lesions that contribute to secondary generalized epileptic encephalopathy; these focal lesions (generally more extended than those of typical focal epilepsy) are usually identified based on interictal iEEG characteristics because of the complicated generalized ictal iEEG discharges. Recent studies have reported successful outcomes of resective epilepsy surgery for children with LGS, despite abundant generalized and multiregional EEG abnormalities (Wyllie *et al* 2007, Lee *et al* 2010a). Although the removal of accurately identified epileptogenic zones does not always guarantee favorable surgical outcomes, additional refinement techniques to confirm the locations of epileptogenic zones would be helpful to avoid failures in resective epilepsy surgery due to the misidentification of epileptogenic zones.

The aim of this study was to investigate whether the frequency domain source imaging of high gamma band (60–100 Hz) iEEG activities prior to ictal onset time could successfully identify epileptogenic zones in secondary generalized epilepsy. To this aim, we applied our approach to iEEG datasets recorded from three successfully operated on LGS patients, and investigated the feasibility of using this approach for pre-surgical evaluation of LGS.

2. Methods

2.1. Patients

Among 27 pediatric patients who had LGS and underwent resective epilepsy surgery during 2001–2007 at Severance Children's Hospital of Korea, 16 patients have been seizure-free since surgery. Four patients without cerebral infarctions or progressive underlying metabolic diseases or chromosomal anomalies were selected among these seizure-free cases. The following four screening criteria were used to select the analysis datasets: (1) up to 30% of preoperative epileptiform discharges were generalized and/or generalized contralateral maximum or multiregional epileptiform discharges; (2) normal or nearly normal brain MRI findings without definite brain lesions including cerebral infarctions, progressive cortical atrophy, or malformation of cortical development; (3) neuroimaging was not helpful in localizing the epileptogenic area; (4) completely seizure-free without any questionable episodes after surgery. Patients who did not satisfy all the above criteria were excluded from the study and the analyses were applied only to the selected patients' iEEG datasets. Three of the four patients whose iEEG recordings showed high gamma oscillations prior to ictal onset time were included in this study (table 1). Parents or guardians of all three LGS patients provided written consent, and the study protocol was approved by the Institutional Review Board of Severance Hospital. Table 1 summarizes the patients' demographic data and characteristics.

The first subject (LYS) was a 3 year old boy with severe mental impairment (Intelligence Quotient (IQ) of 25) who had suffered from refractory epilepsy since 7 months of age. Two types of seizures were observed in this subject, generalized tonic spasms and head drops, and none of the available antiepileptic medications could suppress his seizures. Continuous video-EEG monitoring showed frequent generalized slow spikes and waves and generalized paroxysmal fast activities, as well as localized epileptiform discharges or bisynchronous sharp waves predominantly located in the right frontotemporal areas. Ictal EEG showed generalized slow waves followed by low-voltage fast activity during generalized tonic seizures or head drops, but did not aid in the lateralization of the epileptogenic area. Based on the results of a Phase I study and ictal/interictal iEEG monitoring, the patient underwent a right frontal resection at 3 years of age and was free of seizures for 2.5 years before his seizures recurred at 6 years of age. The posterior margin of the pre-resection site was further resected, and the

Table 1. Patient demographics and characteristics.

Patient	1 (LYS)	2 (JMS)	3 (SWJ)
Age at surgery	3 years	2 years	3 years
Sex	Male	Male	Male
Age at first epilepsy development	7 months	5 months	18 months
Semiology	Generalized tonic spasms and head drops	Head drops and atypical absences	Generalized tonic spasms and staring spells
MRI	Normal	Blurring of the gray–white matter interface on the right frontal lobe	Suspicious but not definite cortical thickening on the right frontal lobe
FDG-PET	Normal	Normal	Focal hypometabolism on the right frontal lobe
Ictal SPECT	Lateralized consistently to the right frontotemporal area	Unsuccessful	Lateralized consistently the right frontotemporal area
Video-EEG	Right frontotemporal area (refer to the text)	Right frontal area (refer to the text)	Right frontotemporal area (refer to the text)
Surgery	(Twice) (1st) Right frontal lobe, (2nd) posterior margin of the pre-resection site	(Once) Right frontal lobe and right anterior temporal lobe	(Twice) (1st) Right frontal lobe, (2nd) right inferior frontal gyrus and right temporal lobe
Outcome	Seizure-free	Seizure-free	Seizure-free
Pathologic result	Focal cortical dysplasia	Focal cortical dysplasia	Focal cortical dysplasia
EEG after operation	Nearly normalized background activities and no epileptiform discharge	Nearly normalized background activities with only occasional multifocal sharp waves	Nearly normalized background activities and no epileptiform discharge
No of subdural electrodes	104	100	116
No of ictal events in iEEG recordings	20	16	19

patient has been free of seizures for 1.6 years (see figure 2 for the surgical resection areas marked on the cortical surface).

The second subject (JMS) was a 2 year old boy with severe mental impairment, who had suffered from refractory epilepsy since 5 months of age. His seizures presented as head drops and were intractable to several available antiepileptic medications. Continuous video-EEG monitoring consistently showed abundant generalized slow spikes and waves and generalized paroxysmal fast activities, as well as localized epileptiform discharges in the right frontal area. Ictal EEG showed generalized slow waves followed by electrodecremental fast activities during head drops, but did not aid in the lateralization of the epileptogenic area. According to the results of a Phase I study and ictal/interictal iEEG monitoring, the right frontal area and right anterior temporal lobe were resected during surgery (see figure 3 for the resection areas marked on the cortical surface). This patient has been free of seizures for 5.6 years without medication.

The third subject (SWJ) was a 3 year old boy with severe mental impairment (IQ of 29) who had developed refractory epilepsy at 18 months of age. This patient presented with two types of seizures, generalized tonic spasms and staring spells, which were not suppressed with available antiepileptic medications. Continuous video-EEG monitoring showed frequent generalized slow spikes and waves, generalized paroxysmal fast activities, and localized

epileptiform discharges or bisynchronous sharp waves in the right frontotemporal areas. Ictal EEG showed generalized slow waves followed by low-voltage fast activities during generalized tonic seizures, but did not aid in the lateralization of the epileptogenic area. Based on the results of a Phase I study and ictal/interictal iEEG monitoring, the patient underwent a right frontal resection when he was 3 years old, which reduced the frequency of his seizures, but did not control them completely. The right inferior frontal gyrus and right temporal area were further resected, and this subject has been free of seizures for 1.6 years on a reduced number of medications (see figure 4 for the final resection areas marked on the cortical surface).

2.2. Determination of surgical resection areas

All subjects were examined using a video-EEG monitoring system with electrodes placed according to the international 10–20 system to define the semiology of habitual seizures and to identify epileptogenic foci. Epileptogenic zones were delineated primarily through interpretation of EEG data. Other imaging modalities such as MRI, PET, and SPECT were used to reinforce these findings. iEEG monitoring using subdural electrodes was also used to determine margins for surgical resection. Preoperative and intraoperative functional mapping and intraoperative electrocorticography were also performed when necessary (Kim *et al* 2009, Lee *et al* 2010b).

The surgical area was defined based on the clinical, neuroimaging, and electrophysiological results. The resection margin for epilepsy of neocortical origin was defined by: (1) the presence of a discrete lesion on MRI and functional neuroimages compatible with ictal or interictal iEEG; (2) various interictal intracranial EEG findings, including more than three repetitive spikes per second, runs of repetitive spike and slow wave discharges, localized or spindle-shaped fast activities and electrodecremental fast activities; and (3) the absence of an eloquent cortex. The diagnosis and classification of pathologic CD was made according to the system described by Palmini and colleagues (Palmini *et al* 2004).

2.3. iEEG data acquisition

Ictal iEEG data were recorded using a multichannel digital EEG acquisition system (Telefactor, Grass Technologies) at a sampling rate of 200 Hz, which was the maximum available sampling rate provided by the system. The locations of the silastic subdural grid and strip electrodes were determined based on multiple neuroimaging data as described above. The recorded iEEG data were reviewed by an epileptologist, and 16 to 20 seizures were observed in each subject (see table 1). Ictal onset times were identified visually by the epileptologist with the aid of video monitoring. No specific pre-processing procedures except for 60 Hz notch filtering were applied to the raw iEEG data.

2.4. Geometric modeling for source imaging

In this study, the realistic geometry boundary element method (BEM) head model was employed for accurate forward calculations. Two-layer tessellated boundary surfaces, consisting of an inner skull boundary and epicortical surface, were generated using CURRY6 for Windows (Compumedics Neuroscan, EI Paso, TX, USA). Surface nodes and boundary elements were generated from T1-weighted MR images of each LGS patient. There were 4167, 3609, and 3593 boundary nodes for subjects JMS, LYS, and SWJ, respectively. The locations of subdural grid electrodes were extracted from each patient's CT images and co-registered on the epicortical surface of the BEM model. Conductivity values of 1.79 and 0.33 S m^{-1} were

used for the CSF and brain compartments, respectively (Oostendorp *et al* 2000). The volume conduction effect outside the inner skull boundary was ignored due to the very low electrical conductivity of the human skull layer (Fuchs *et al* 2007). A first-order, node-based BEM was used for the construction of a leadfield matrix (Fuchs *et al* 2007).

Because synchronously activated pyramidal cortical neurons are believed to be the main EEG and MEG generators, many recent studies have adopted this physiological phenomenon as a basic anatomical constraint in EEG or MEG source imaging (Dale and Sereno 1993, Kincses *et al* 1999, Dale *et al* 2000, Babiloni *et al* 2003, 2005). Numerous dipolar sources were placed on the cortical surface that was also tessellated using CURRY6 to impose this anatomical constraint. The numbers of cortical surface vertices generated for subjects JMS, LYS, and SWJ were 12 565, 13 543, and 13 791, respectively.

2.5. iEEG spectrogram evaluation

In this study, the short-time Fourier transform (STFT) was used to determine the time interval with high gamma band activity (60–100 Hz) prior to ictal onset time. The time domain iEEG signals were transformed into frequency domains using the STFT over the 1–100 Hz frequency range with a frequency resolution of 0.78 Hz. For the STFT calculation, a 'spectrogram' function implemented in MATLAB 2009a (Mathworks, Inc., USA) was used. A Hamming window with 256 data samples and a 75% overlapping rate was applied for the spectrogram evaluation in order to reduce spectral leakage. A time interval for the frequency domain source imaging was selected for each event based on visual inspection of the spectrogram. Since the length of the time interval containing high gamma band activity before ictal onset time was not longer than 256 time samples in any case (see figures 2–4), the size of the analysis window for the frequency domain source imaging was fixed at 256 time samples.

Since many recent studies have demonstrated that cortical areas with high gamma oscillation occurring before the start of an epileptic seizure are closely associated with epileptogenic zones (Fisher *et al* 1992, Traub *et al* 2001, Worrell *et al* 2004), each ictal event was inspected to determine if it included any time interval with a distinct increase in high gamma band activity before the ictal onset time. Four ictal events were selected for LYS and JMS, and two ictal events were selected for SWJ. For each of the selected ictal events, the position of the analysis time window was determined to include a time interval with increased high gamma band activity (see figure 1).

2.6. Frequency domain source imaging

The fast Fourier transform (FFT) was applied to time domain iEEG signals $\boldsymbol{x}(t)$ over a 1–100 Hz frequency range, resulting in frequency domain signals $\mathbf{X}(f)$ with a frequency resolution of approximately 0.78 Hz. Then, the real part $\boldsymbol{q}_j(f_i)_{\mathrm{Re}}$ and imaginary part $\boldsymbol{q}_j(f_i)_{\mathrm{Im}}$ of the current source vector at the jth cortical vertex with respect to the frequency of interest f_i were evaluated by applying frequency domain minimum norm estimation (FD-MNE) (Lin *et al* 2004, Im *et al* 2007) to the Fourier transformed signals $\mathbf{X}(f_i)_{\mathrm{Re}}$ and $\mathbf{X}(f_i)_{\mathrm{Im}}$, where Re and Im represent the real and imaginary parts of the Fourier transformed signals, respectively.

The MNE algorithm is based on the L2-norm minimization, and the general form of the function to be minimized can be expressed as

$$\min\left\{\|\mathbf{L}\mathbf{J}-\mathbf{x}\|_2^2+\lambda\|\mathbf{W}\mathbf{J}\|_2^2\right\}, \tag{1}$$

where $\mathbf{L}$ is an $m \times n$ leadfield matrix that relates m sensors and n sources, $\mathbf{J}$ is a $3n \times 1$ source vector, $\|\cdot\|_2$ represents the Euclidean L2 norm, λ is a regularization parameter that controls the weight given to the minimization of the side constraint, and $\mathbf{W}$ is a diagonal

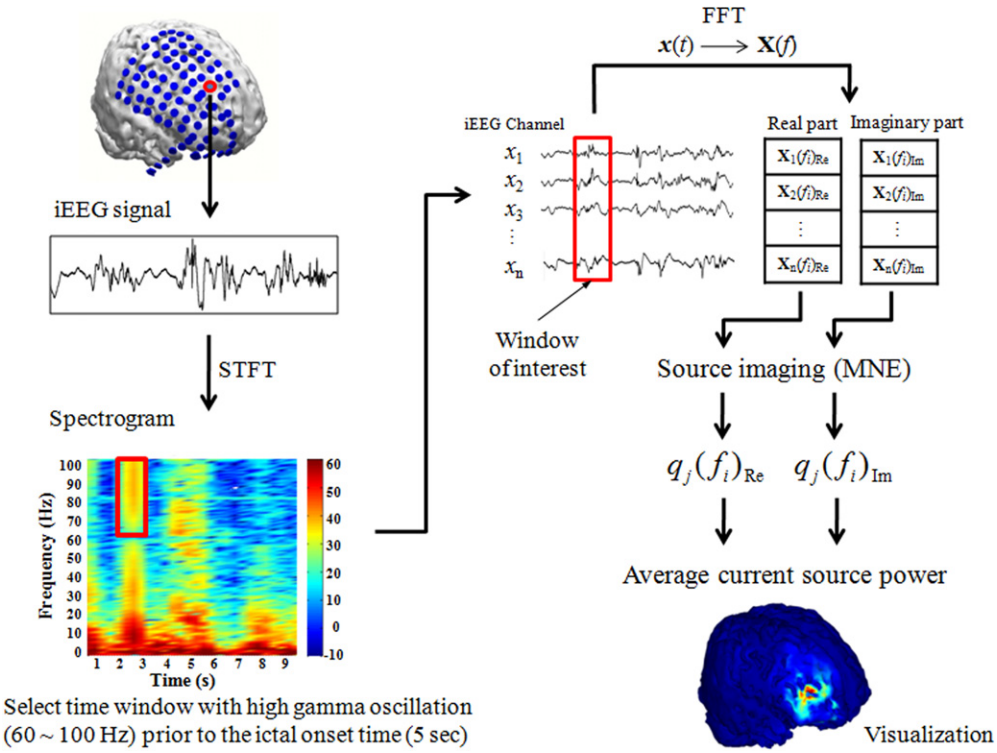

Figure 1. A schematic illustration of the study procedures. First, a time segment containing the time of ictal onset was selected from the iEEG recordings. An analysis time window was determined by inspecting the increase in high gamma activity (60–100 Hz) prior to the ictal onset time using time–frequency analysis (spectrogram). In the time–frequency spectrogram, the (red) box indicates the selected time window (size = 256 time samples). The signals in this time window $\mathbf{x}(t)$ were transformed into frequency domain signals $\mathbf{X}(f)$ using the FFT. The MNE was then applied to the real and imaginary parts of the Fourier-transformed signals. Finally, the average current source power at the jth cortical vertex was estimated from the MNE results and displayed on the tessellated cortical surface.

weighting matrix that was used to compensate the depth dependence of MNE. In the CURRY software package, depth normalization is automatically applied according to the processes described in a paper by Fuchs *et al* (1999) (please refer to equations 10 and 11 in the article). CURRY6 software was used for the cortical source imaging and exported the resultant source distributions $\boldsymbol{q}_j(f_i)_{\mathrm{Re}}$ and $\boldsymbol{q}_j(f_i)_{\mathrm{Im}}$ to an ASCII data file for further analyses. The regularization parameter was determined automatically using the χ^2 criterion algorithm implemented in the CURRY software. The average current source power at the jth cortical vertex with respect to the frequency band of interest was then estimated as

$$Q_j = \frac{1}{M}\sum_{i=1}^{M}\left\{q_j(f_i)^2_{\mathrm{Re}} + q_j(f_i)^2_{\mathrm{Im}}\right\}, \tag{2}$$

where M represents the number of discrete frequency samples in high gamma band (60–100 Hz). The 60 Hz (power line frequency) and 100 Hz frequencies were excluded from the analysis. In patients LYS and SWJ, 80 Hz was also excluded as unwanted noise components were observed. The distribution of the average current source powers was then visualized on the tessellated cortical surface using Matlab. Figure 1 illustrates the overall analysis procedures.

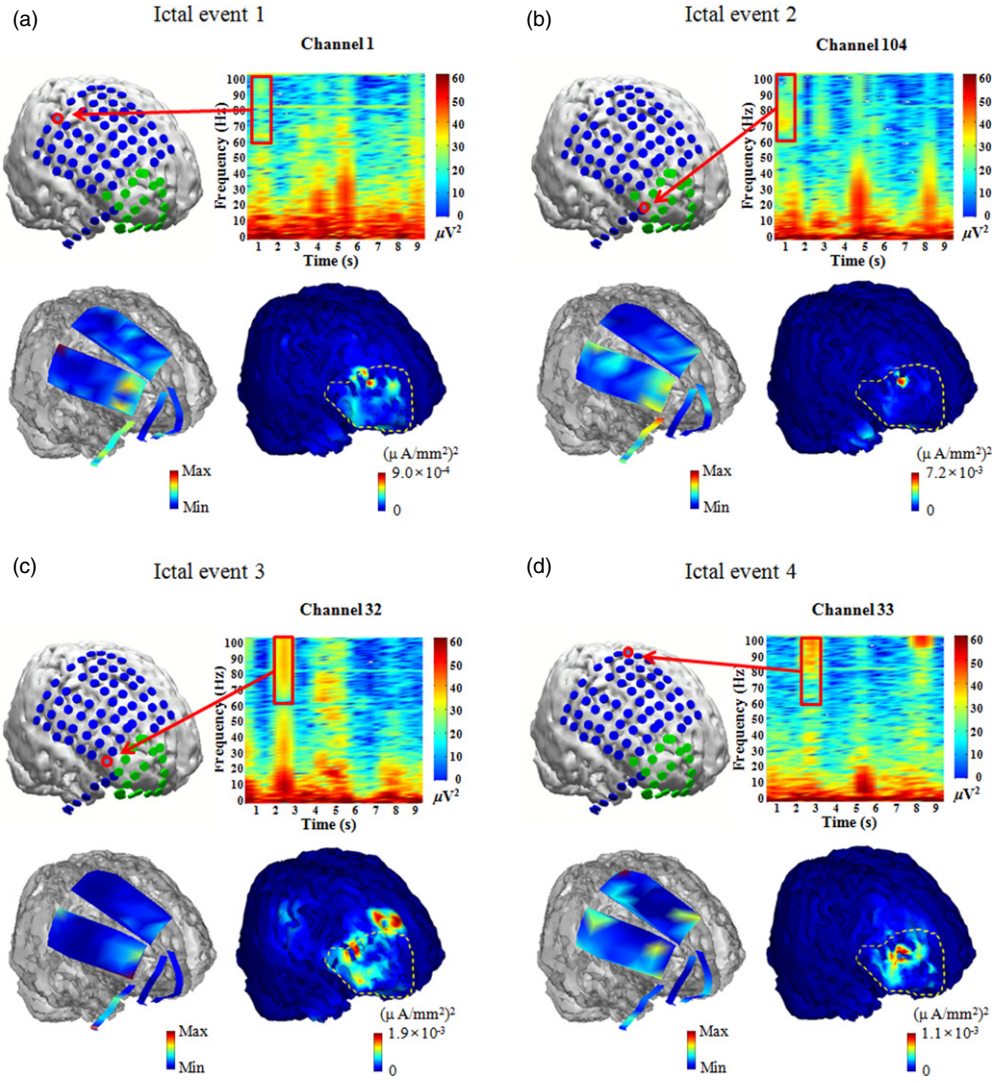

Figure 2. Analysis results for patient 1 (LYS). Figures (a), (b), (c), and (d) show analysis results for different ictal events. In each of the figures (a)–(d), the upper-left image depicts the locations of the patient's subdural electrodes and the surgical resection area marked on the subdural electrodes is shown in (green). In this figure, a (red) circle indicated by a (red) arrow represents the channel with the highest averaged high-gamma power value in the analysis time window. The time–frequency spectrogram of an iEEG signal recorded on this channel is illustrated in the upper-right image, where the (red) rectangular box indicates the selected analysis time window that showed increased high gamma activity prior to ictal onset time. The lower-left image shows an averaged high gamma power distribution on the sensor plane and the lower-right image shows a cortical source distribution resulting from frequency domain source imaging. In the lower-left image, the (yellow) dashed line represents the actual surgical resection area.

3. Results

Figures 2–4 illustrate the overall analysis results for the three LGS patients (LYS, JMS, and SWJ), respectively. The position of subdural electrodes, surgical resection areas, time–frequency map, sensor-level high gamma power distribution, and cortical source distribution

are illustrated in each of these figures. For example, the upper-left image in figure 2(a) depicts the locations of the patient's subdural electrodes and the surgical resection area is marked on the subdural electrodes in green. In this figure, a red circle indicated by a red arrow represents the channel that has the highest averaged high-gamma power value in the analysis time window. The time–frequency spectrogram of an iEEG signal recorded at this channel is illustrated in the upper-right image, where the red rectangular box indicates the selected analysis time window that showed increased high gamma activity prior to ictal onset (centered at 5 s in all cases). The lower-left figure shows an averaged high gamma power distribution on the sensor plane and the lower-right figure shows a cortical source distribution resulting from frequency domain source imaging. In the cortical source distribution, the yellow dashed line represents the actual surgical resection area.

In patient 1 (LYS), four ictal events included visually distinct high gamma activities prior to the ictal onset time (figures 2(a)–(d)). As seen from the images in figure 2, the results of the frequency domain source imaging coincided much better with the surgical resection areas than those of the sensor-level analyses. In the case of ictal events 1 (figure 2(a)) and 4 (figure 2(d)), the results of the sensor-level analyses contained several electrodes with strong high gamma spectral powers located far from the surgical resection area, while the cortical source activities were concentrated mostly inside the surgical resection area. Some spurious source activities were observed outside the surgical resection areas in the source imaging results of ictal event 3 (figure 2(c)), but their locations were not far from the surgical resection area.

In patient 2 (JMS), four ictal events included visually distinct high gamma activities prior to the ictal onset time (figures 3(a)–(d)). As shown in figure 3, the results of the frequency domain source localization coincided well with the surgical resection areas. As in the previous case, the results of frequency domain source imaging coincided much better with the surgical resection areas than those of the sensor-level analyses. In the time–frequency spectrogram of ictal event 1, increased high gamma band activity was also observed during the 1 to 2 s time interval. However, the high gamma oscillations around 1.5 s disappeared when a common average reference was applied, which implies that they were common noise components. On the other hand, since the selected time interval marked with a red box in figure 3(a) did not disappear after the re-referencing, it was selected for the source imaging. The accuracy of estimating epileptogenic zones was considerably enhanced by using the frequency domain source imaging in most cases, but the results of the sensor-level analysis and frequency domain source imaging were not very different in the cases of ictal events 2 (figure 3(b)) and 3 (figure 3(c)). In these two cases, both the sensor-level results and the source distributions commonly contained high gamma band activities around the sensorimotor cortex. Indeed, this area was also initially considered the resection area, but it was excluded in the final surgery plan as the resection of this area might significantly impair the patient's motor function.

In patient 3 (SWJ), two ictal events exhibited visually discriminable high gamma activities prior to the time of ictal onset (figure 4). In this case, both the sensor-level results and the source distributions coincided fairly well with the surgical resection areas. In ictal event 2 (figure 4(b)), source activities were distributed only around the posterior dorsolateral prefrontal cortex. This seems to be because fewer numbers of subdural grid electrodes were placed in the frontal cortex compared to the previous two patients.

4. Discussion

This study examined the feasibility of using frequency domain source imaging of high gamma band activity to estimate epileptogenic zones in pediatric patients with LGS. For the three LGS patients considered in this study, high gamma cortical source distributions coincided well with

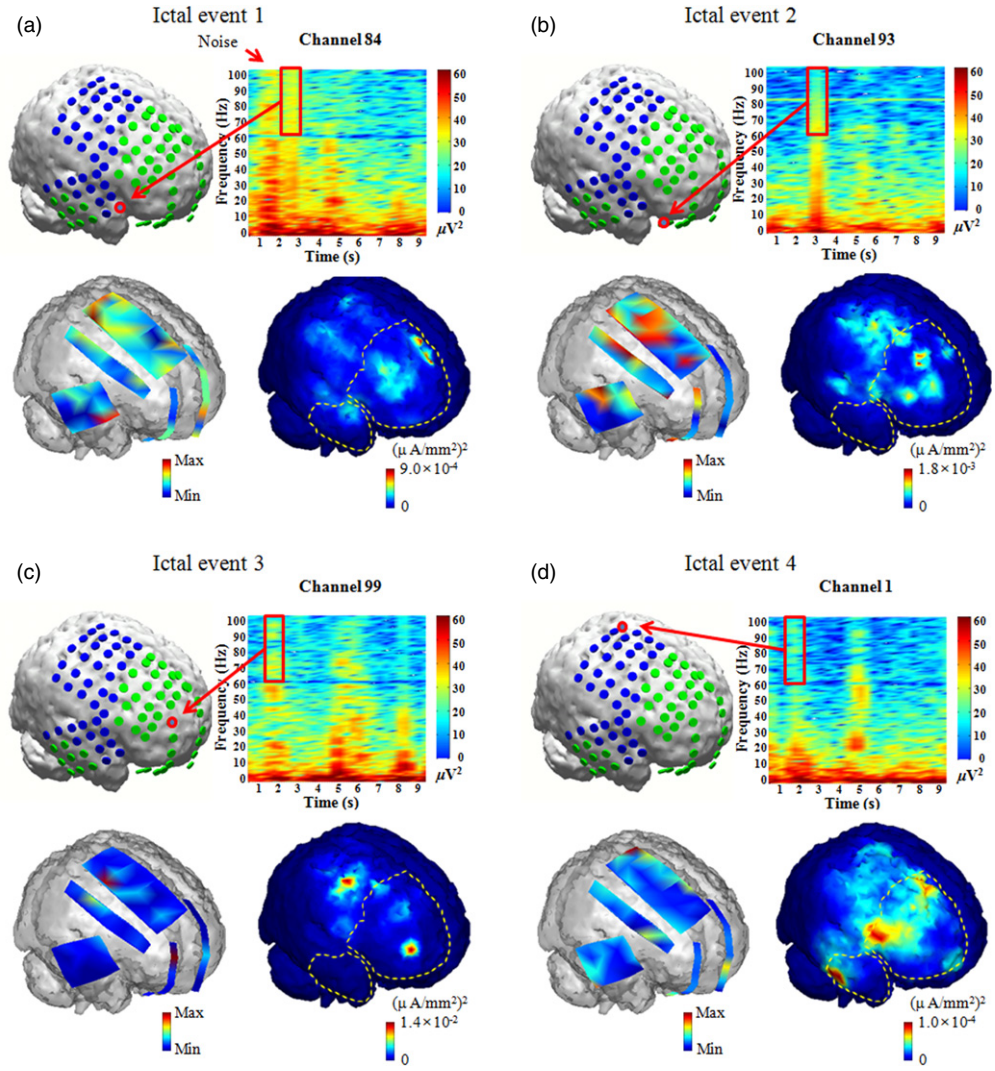

Figure 3. Analysis results for patient 2 (JMS). Figures (a), (b), (c), and (d) show the analysis results for different ictal events. Please refer to figure 2 caption.

the surgical resection areas determined by well-experienced epileptologists. Moreover, most spurious activities that appeared in the sensor-level spectral analysis were not observed in the frequency domain source imaging results, suggesting that frequency domain source imaging of ictal iEEG might provide useful auxiliary information for successful epilepsy surgery in patients with LGS.

4.1. Frequency domain EEG and MEG source imaging

In EEG and MEG studies, frequency domain source imaging has already become a well-established tool to estimate brain regions where epileptiform activities are generated (Lantz *et al* 1999, Worrell *et al* 2000, Xiang *et al* 2009) as well as to investigate human brain

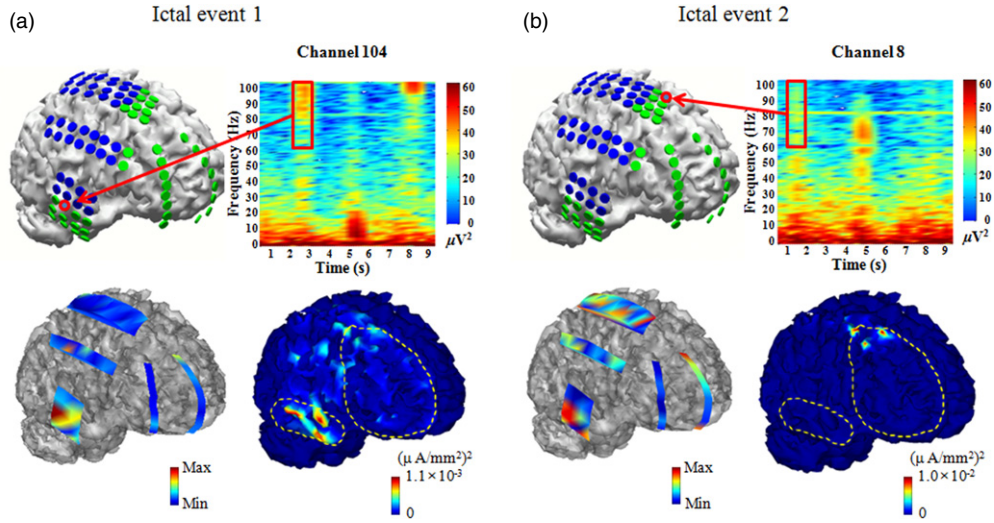

Figure 4. Analysis results for patient 3 (SWJ). Figures (a) and (b) show the analysis results for different ictal events. Please refer to figure 2 caption.

functions (Lin *et al* 2004, Liljeström *et al* 2005, Im *et al* 2007, Yuan *et al* 2008, Dalal *et al* 2008). Lantz *et al* (1999) reported that frequency domain EEG source localization using the equivalent current dipole (ECD) model provided reproducible results for seizures originating from the mesial temporal area. They used peak spectral frequencies between 0.5 and 35 Hz to localize ECDs in the frequency domain. Worrell *et al* (2000) showed that phase-encoded spectral analysis with a frequency range between 1 and 35 Hz, combined with low-resolution electromagnetic tomography, could be a promising method for investigating the complex spatiotemporal dynamics of ictal discharges. Xiang *et al* (2009) demonstrated that MEG can also be helpful in recording HFO, and the results of MEG source imaging of HFO were concordant with those of iEEG. As mentioned previously, frequency domain source imaging of HFO using iEEG data had not been reported before.

4.2. iEEG source imaging

In contrast to EEG and MEG source imaging studies that have a long history of investigation, the first investigations of iEEG source imaging did not start until 2007. Fuchs *et al* (2007) first suggested the possibility of using iEEG for estimating cortical source activities. In their study, MNE was applied to both simulated and recorded iEEG datasets, the results of which demonstrated that iEEG source imaging can localize cortical sources with fairly high accuracy. Zhang *et al* (2008) showed that iEEG source imaging could localize deep brain sources better than traditional EEG source imaging. Dümpelmann *et al* (2009) compared the localization accuracies of two different iEEG source imaging methods, multiple signal classification (MUSIC) and MNE, and reported that MUSIC performed better than MNE when sources were located in relatively deep brain areas. Cho *et al* (2011) recently performed a simulation study investigating which algorithm is most appropriate for accurate iEEG source imaging. Interestingly, the simulation results showed that the traditional MNE algorithm outperformed the other imaging algorithms, particularly in cases when larger-sized sources were activated. The MNE algorithm was selected for the present iEEG source imaging study because the

epileptogenic zones of secondary generalized epilepsy have relatively more widespread distributions than those of focal epilepsy.

4.3. Secondary generalized epilepsy

It is noteworthy that most previous studies on iEEG source imaging focused on the localization of epileptogenic zones in focal epilepsy. However, in some patients with secondary generalized epilepsy such as LGS, the localization of epileptogenic zones is also critical for surgical treatment, as a number of recent studies have demonstrated that some focal epileptogenic zones are likely to generate generalized epileptiform discharges in many types of generalized epilepsy (Berman *et al* 2010, Bai *et al* 2010). It is generally more difficult to localize epileptogenic zones in secondary generalized epilepsy than in focal epilepsy because of its generalized iEEG discharges during seizure. In this study, the surgical resection areas were determined using multiple neuroimaging modalities as presented in table 1. However, as seen in the table, some traditional neuroimaging modalities did not effectively identify the epileptogenic areas, e.g. FDG-PET in patients LYS and JMS and ictal SPECT in patient JMS. Moreover, the results from interictal video-EEG monitoring indicated only rough locations of the epileptogenic zones, and ictal EEG recorded during generalized tonic seizures or head drops did not aid in lateralization of the epileptogenic zones in any of the patients. Even after visual inspection of the iEEG signals, two of the three patients underwent resective surgeries twice because their seizures recurred after the first operation, which indirectly illustrates the need to introduce new additional modalities for more reliable pre-surgical evaluation.

Recently, our group introduced several computational iEEG analysis methods for the localization of epileptogenic zones in LGS (Jung *et al* 2011, Cho *et al* 2012). Although these studies demonstrated the possibility of using computational iEEG analysis in the pre-surgical evaluation of patients with LGS, the previous results were not only confined to the intracranial sensor plane, but were also contaminated with abundant spurious source activities. This study proposes an alternative approach for the localization of epileptogenic zones in LGS by mapping the sensor-level potential distributions to the cortex-level source activities. This approach may also be a useful tool for the estimation of epileptogenic zones in secondary generalized epilepsy including LGS. Although the frequency domain iEEG source imaging was only applied to iEEG data acquired from LGS patients, hopefully this method can also be applied to iEEG data recorded from patients with focal epilepsy in future studies.

4.4. Limitations and future prospects

This study used a BEM model to solve forward problems because it provides a reasonable compromise between accuracy and computational cost (Fuchs *et al* 2007, Plummer *et al* 2010). According to reports by Zhang *et al* (2008) and Rullmann *et al* (2009), the use of the finite element method (FEM) enables consideration of anisotropic brain tissue conductivity as well as nonconductive silastic base pads. Further studies are needed to address the difficulties in modeling and to reduce the high computational costs so that FEM models can be practically applied to clinical iEEG analyses.

HFO, the frequency range of which exceeds 100 Hz, has been actively studied in recent years (Engel Jr *et al* 2009). HFOs with a frequency range between 100 and 500 Hz were initially recorded in animals using a single unit recording system, but recently they have been recorded using both depth and subdural electrodes in humans. A frequency band between 100 and 250 Hz is generally called a ripple and a frequency band between 250 and 500 Hz is called a fast ripple. Several recent studies have shown that these high frequency signals are

also closely associated with epileptogenic zones (Bragin *et al* 1999, 2002, Jirsch *et al* 2006, Ochi *et al* 2007, Staba *et al* 2007, Worrell *et al* 2008, Jacobs *et al* 2010, Zijlmans *et al* 2011). Unfortunately, however, due to the limited sampling frequency of the present iEEG data, it was not possible to extend this study to these high frequency bands. Since iEEG recordings with higher sampling rates would allow for the analysis of ripple and fast ripple, our group recently started to collect iEEG datasets with much higher sampling rate, with the hope of applying our approach to higher frequency band iEEG data analyses.

iEEG data from only three LGS patients were used in this study because it was difficult to obtain iEEG datasets for LGS patients who had undergone successful epilepsy surgery and did not have cerebral infarctions or progressive underlying metabolic diseases. In future studies, more extensive computational iEEG analyses using massive clinical epilepsy iEEG data should be performed to quantitatively compare the performances of various neuroimaging modalities used for the delineation of epileptogenic zones. In addition to the current analyses applied only to LGS patients with successful surgical outcomes, it would be interesting to apply this study approach to a larger sample of patients who were not seizure-free after the resective epilepsy surgery. This would make it possible to investigate whether the epileptogenic zones localized by our approach were not completely removed during epilepsy surgery in patients with unfavorable surgical outcomes. Kim *et al* (2010) recently demonstrated the possibility of localizing ictal epileptogenic zones that are located outside the grid electrode surfaces using ECD source localization applied to ictal iEEG data acquired from partial epilepsy patients. However, no studies have attempted to apply the iEEG extended source imaging approach to similar cases, which is also a promising research topic that should be investigated in future studies.

Acknowledgments

This work was supported in part by the KRISS-WCL project (Development of Measurement Technology for Cognitive Process) and in part by the Public Welfare and Safety Research Program through the National Research Foundation of Korea (NRF) funded by the Ministry of Education, Science and Technology (no 2011-0027859).

References

Alarcon G, Binnie C D, Elwes R D C and Polkey C E 1995 Power spectrum and intracranial EEG patterns at seizure onset in partial epilepsy *Electroencephalogr. Clin. Neurophysiol.* **94** 326–37

Allen P J, Fish D R and Smith S J M 1992 Very high-frequency rhythmic activity during SEEG suppression in frontal lobe epilepsy *Electroencephalogr. Clin. Neurophysiol.* **82** 155–9

Babiloni F, Babiloni C, Carducci F, Romani G L, Rossini P M, Angelone L M and Cincotti F 2003 Multimodal integration of high-resolution EEG and functional magnetic resonance imaging data: a simulation study *NeuroImage* **19** 1–15

Babiloni F *et al* 2005 Estimation of the cortical functional connectivity with the multimodal integration of high-resolution EEG and fMRI data by directed transfer function *NeuroImage* **24** 118–31

Bai X, Vestal M, Berman R, Negishi M, Spann M, Vega C, DeSalvo M N, Novotny E, Constable R T and Blumenfeld H 2010 Dynamic timecourse of typical childhood absence seizures: EEG, behavior and fMRI *J. Neurosci.* **30** 5884–93

Behrens E, Zentner J, Van Roost D, Hufnagel A, Elger C E and Schramm J 1994 Subdural and depth electrodes in the presurgical evaluation of epilepsy *Acta Neurochir.* **128** 84–7

Berman R *et al* 2010 Simultaneous EEG, fMRI, and behavioral testing in typical childhood absence seizures *Epilepsia* **51** 2011–22

Binnie C D, Elwes R D C, Polkey C E and Volans A 1994 Utility of stereoelectroencephalography in preoperative assessment of temporal lobe epilepsy *J. Neurol. Neurosurg. Psychiatry* **57** 58–65

Boling W, Aghakhani Y, Andermann F, Sziklas V and Olivier A 2009 Surgical treatment of independent bitemporal lobe epilepsy defined by invasive recordings *J. Neurol. Neurosurg. Psychiatry* **80** 533–8

Bragin A, Engel J Jr, Wilson C L, Fried I and Mathern G W 1999 Hippocampal and entorhinal cortex high-frequency oscillations (100–500 Hz) in human epileptic brain and in kainic acid-treated rats with chronic seizures *Epilepsia* **40** 127–37

Bragin A, Wilson C L, Staba R J, Reddick M, Fried I and Engel J Jr 2002 Interictal high-frequency oscillations (80–500 Hz) in the human epileptic brain: entorhinal cortex *Ann. Neurol.* **52** 407–15

Cho J H, Hong S B, Jung Y J, Kang H C, Kim H D, Suh M, Jung K Y and Im C H 2011 Evaluation of algorithms for intracranial EEG (iEEG) source imaging of extended sources: feasibility of using iEEG source imaging for localizing epileptogenic zones in secondary generalized epilepsy *Brain Topogr.* **24** 91–104

Cho J H, Kang H C, Jung Y J, Lee Y H, Kim H D and Im C H 2012 Localization of ictal onset zones in Lennox–Gastaut syndrome (LGS) based on information theoretical time delay analysis of intracranial electroencephalography (iEEG) *Epilepsy Res.* **99** 78–86

Dalal S S *et al* 2008 Five-dimensional neuroimaging: localization of the time–frequency dynamics of cortical activity *NeuroImage* **40** 1686–700

Dale A M, Liu A K, Fischl B R, Buckner R L, Belliveau J W, Lewine J D and Halgren E 2000 Dynamic statistical parametric mapping: combining fMRI and MEG for high-resolution imaging of cortical activity *Neuron* **26** 55–67

Dale A M and Sereno M I 1993 Improved localization of cortical activity by combining EEG and MEG with MRI cortical surface reconstruction: a linear approach *J. Cogn. Neurosci.* **5** 162–76

Ding L, Worrell G A, Lagerlund T D and He B 2007 Ictal source analysis: localization and imaging of causal interactions in humans *NeuroImage* **34** 575–86

Dubeau F and McLachlan R S 2000 Invasive electrographic recording techniques in temporal lobe epilepsy *Can. J. Neurol. Sci.* **27** S29–34

Dümpelmann M, Ball T and Schulze-Bonhage A 2012 sLORETA allows reliable distributed source reconstruction based on subdural strip and grid recordings *Hum. Brain Mapp.* **33** 1172–88

Dümpelmann M, Fell J, Wellmer J, Urbach H and Elger C E 2009 3D source localization derived from subdural strip and grid electrodes: a simulation study *Clin. Neurophysiol.* **120** 1061–9

Engel J Jr, Bragin A, Staba R and Mody I 2009 High-frequency oscillations: what is normal and what is not? *Epilepsia* **50** 598–604

Fisher R S, Webber W R S, Lesser R P, Arroyo S and Uematsu S 1992 High-frequency EEG activity at the start of seizures *J. Clin. Neurophysiol.* **9** 441–8

Fuchs M, Wagner M and Kastner J 2007 Development of volume conductor and source models to localize epileptic foci *J. Clin. Neurophysiol.* **24** 101–19

Fuchs M, Wagner M, Kohler T and Wischmann H-A 1999 Linear and nonlinear current density reconstructions *J. Clin. Neurophysiol.* **16** 267–95

Heiskala H 1997 Community-based study of Lennox–Gastaut syndrome *Epilepsia* **38** 526–31

Im C H, Hwang H J, Che H and Lee S 2007 An EEG-based real-time cortical rhythmic activity monitoring system *Physiol. Meas.* **28** 1101–13

Jacobs J, Zijlmans M, Zelmann R, Chatillon C E, Hall J, Olivier A, Dubeau F and Gotman J 2010 High-frequency electroencephalographic oscillations correlate with outcome of epilepsy surgery *Ann. Neurol.* **67** 209–20

Jirsch J D, Urrestarazu E, LeVan P, Olivier A, Dubeau F and Gotman J 2006 High-frequency oscillations during human focal seizures *Brain* **129** 1593–608

Jung Y J, Kang H C, Choi K O, Lee J S, Kim D S, Cho J H, Kim S H, Im C H and Kim H D 2011 Localization of ictal onset zones in Lennox–Gastaut syndrome using directional connectivity analysis of intracranial electroencephalography *Seizure* **20** 449–57

Kim J S, Im C H, Jung Y J, Kim E Y, Lee S K and Chung C K 2010 Localization and propagation analysis of ictal source rhythm by electrocorticography *NeuroImage* **52** 1279–88

Kim J T, Bai S J, Choi K O, Lee Y J, Park H J, Kim D S, Kim H D and Lee J S 2009 Comparison of various imaging modalities in localization of epileptogenic lesion using epilepsy surgery outcome in pediatric patients *Seizure* **18** 504–10

Kim Y K, Lee D S, Lee S K, Chung C K, Chung J K and Lee M C 2002 ^{18}F-FDG PET in localization of frontal lobe epilepsy: comparison of visual and SPM analysis *J. Nucl. Med.* **43** 1167–74

Kincses W E, Braun C, Kaiser S and Elbert T 1999 Modeling extended sources of event-related potentials using anatomical and physiological constraints *Hum. Brain Mapp.* **8** 182–93

Kobayashi K, Inoue T, Watanabe Y, Oka M, Endoh F, Yoshinaga H and Ohtsuka Y 2009 Spectral analysis of EEG gamma rhythms associated with tonic seizures in Lennox–Gastaut syndrome *Epilepsy Res.* **86** 15–22

Krakow K *et al* 1999 EEG-triggered functional MRI of interictal epileptiform activity in patients with partial seizures *Brain* **122** 1679–88

Lantz G, Michel C M, Seeck M, Blanke O, Landis T and Rosén I 1999 Frequency domain EEG source localization of ictal epileptiform activity in patients with partial complex epilepsy of temporal lobe origin *Clin. Neurophysiol.* **110** 176–84

Lee Y J *et al* 2010a Comparison of temporal lobectomies of children and adults with intractable temporal lobe epilepsy *Childs Nerv. Syst.* **26** 177–83

Lee Y J, Kang H C, Lee J S, Kim S H, Kim D S, Shim K W, Lee Y H, Kim T S and Kim H D 2010b Resective pediatric epilepsy surgery in Lennox–Gastaut syndrome *Pediatrics* **125** 58–66

Liljeström M, Kujala J, Jensen O and Salmelin R 2005 Neuromagnetic localization of rhythmic activity in the human brain: a comparison of three methods *NeuroImage* **25** 734–45

Lin F H, Witzel T, Hämäläinen M S, Dale A M, Belliveau J W and Stufflebeam S M 2004 Spectral spatiotemporal imaging of cortical oscillations and interactions in the human brain *NeuroImage* **23** 582–95

Mars N J I and Lopes da Silva F H 1987 EEG analysis methods based on information theory *Methods of Analysis of Brain Electrical and Magnetic Signals: EEG Handbook* ed A S Gevins and A Remond (Amsterdam: Elsevier) pp 279–307

Ochi A *et al* 2007 Dynamic changes of ictal high-frequency oscillations in neocortical epilepsy: using multiple band frequency analysis *Epilepsia* **48** 286–96

Oliveira A J, da Costa J C, Hilário L N, Anselmi O E and Palmini A 1999 Localization of the epileptogenic zone by ictal and interictal SPECT with ^{99m}Tc-ethyl cysteinate dimer in patients with medically refractory epilepsy *Epilepsia* **40** 693–702

Oostendorp T F, Delbeke J and Stegeman D F 2000 The conductivity of the human skull: results of *in vivo* and *in vitro* measurements *IEEE Trans. Biomed. Eng.* **47** 1487–92

Palmini A *et al* 2004 Terminology and classification of the cortical dysplasias *Neurology* **62** S2–8

Plummer C, Wagner M, Fuchs M, Vogrin S, Litewka L, Farish S, Bailey C, Harvey A S and Cook M J 2010 Clinical utility of distributed source modelling of interictal scalp EEG in focal epilepsy *Clin. Neurophysiol.* **121** 1726–39

Pondal-Sordo M, Diosy D, Téllez-Zenteno J F, Sahjpaul R and Wiebe S 2007 Usefulness of intracranial EEG in the decision process for epilepsy surgery *Epilepsy Res.* **74** 176–82

Prasad A, Pacia S V, Vazquez B, Doyle W K and Devinsky O 2003 Extent of ictal origin in mesial temporal sclerosis patients monitored with subdural intracranial electrodes predicts outcome *J. Clin. Neurophysiol.* **20** 243–8

Rampp S, Kaltenhäuser M, Weigel D, Buchfelder M, Blümcke I, Dörfler A and Stefan H 2010 MEG correlates of epileptic high gamma oscillations in invasive EEG *Epilepsia* **51** 1638–42

Rosenow F and Lüders H 2001 Presurgical evaluation of epilepsy *Brain* **124** 1683–1700

Rullmann M, Anwander A, Dannhauer M, Warfield S K, Duffy F H and Wolters C H 2009 EEG source analysis of epileptiform activity using a 1 mm anisotropic hexahedra finite element head model *NeuroImage* **44** 399–410

Staba R J, Frighetto L, Behnke E J, Mathern G W, Fields T, Bragin A, Ogren J, Fried I, Wilson C L and Engel J Jr 2007 Increased fast ripple to ripple ratios correlate with reduced hippocampal volumes and neuron loss in temporal lobe epilepsy patients *Epilepsia* **48** 2130–8

Swiderski B, Osowski S, Cichocki A and Rysz A 2009 Single-class SVM and directed transfer function approach to the localization of the region containing epileptic focus *Neurocomputing* **72** 1575–83

Traub R D, Whittington M A, Buhl E H, LeBeau F E N, Bibbig A, Boyd S, Cross H and Baldeweg T 2001 A possible role for gap junctions in generation of very fast EEG oscillations preceding the onset of, and perhaps initiating, seizures *Epilepsia* **42** 153–70

Wilke C, Van Drongelen W, Kohrman M and He B 2010 Neocortical seizure foci localization by means of a directed transfer function method *Epilepsia* **51** 564–72

Worrell G A, Gardner A B, Stead S M, Hu S, Goerss S, Cascino G J, Meyer F B, Marsh R and Litt B 2008 High-frequency oscillations in human temporal lobe: simultaneous microwire and clinical macroelectrode recordings *Brain* **131** 928–37

Worrell G A, Lagerlund T D, Sharbrough F W, Brinkmann B H, Busacker N E, Cicora K M and O'Brien T J 2000 Localization of the epileptic focus by low-resolution electromagnetic tomography in patients with a lesion demonstrated by MRI *Brain Topogr.* **12** 273–82

Worrell G A, Parish L, Cranstoun S D, Jonas R, Baltuch G and Litt B 2004 High-frequency oscillations and seizure generation in neocortical epilepsy *Brain* **127** 1496–506

Wu J Y *et al* 2006 Magnetic source imaging localizes epileptogenic zone in children with tuberous sclerosis complex *Neurology* **66** 1270–2

Wyllie E, Lachhwani D K, Gupta A, Chirla A, Cosmo G, Worley S, Kotagal P, Ruggieri P and Bingaman W E 2007 Successful surgery for epilepsy due to early brain lesions despite generalized EEG findings *Neurology* **69** 389–97

Xiang J *et al* 2009 Frequency and spatial characteristics of high-frequency neuromagnetic signals in childhood epilepsy *Epileptic Disord.* **11** 113–25

Yuan H, Doud A, Gururajan A and He B 2008 Cortical imaging of event-related (de)synchronization during online control of brain–computer interface using minimum-norm estimates in frequency domain *IEEE Trans. Neural Syst. Rehabil. Eng.* **16** 425–31

Zhang Y C, van Drongelen W, Kohrman M and He B 2008 Three-dimensional brain current source reconstruction from intra-cranial ECoG recordings *NeuroImage* **42** 683–95

Zijlmans M, Jacobs J, Kahn Y U, Zelmann R, Dubeau F and Gotman J 2011 Ictal and interictal high frequency oscillations in patients with focal epilepsy *Clin. Neurophysiol.* **122** 664–71